ELSEVIER

X-ray initiated molecular photochemistry of Cl-containing adsorbates on a Si(100) surface using synchrotron radiation

J.M. Chen [a,*], K.T. Lu [a], J.M. Lee [a,b], S.C. Haw [a]

[a] *National Synchrotron Radiation Research Center, Hsinchu 30076, Taiwan, ROC*
[b] *Department of Electrophysics, National Chiao Tung University, Hsinchu, Taiwan, ROC*

Abstract

X-ray initiated molecular photochemistry for $SiCl_4$ and CCl_4 adsorbed on Si(100) at ∼90 K following Cl 2p core-level excitation is investigated by photon stimulated ion desorption and ion kinetic energy distribution measurements. The Cl 2p → $8a_1^*$ excitation of solid $SiCl_4$ induces the significant enhancement (∼900%) of the Cl^+ yield, while the Cl 2p → $7a_1^*$ excitation of condensed CCl_4 leads to a moderate enhancement (∼500%) of the Cl^+ yield. The enhancement of Cl^+ yield at the specific core-excited states is strongly correlated to the ion escaped energy. Upon X-ray exposure for CCl_4 adsorbed on Si(100) (20-L exposure), the Cl^+ yields at $7a_1^*$ resonances decrease and new structures at higher photon energies are observed. Cl^+ yields at these new resonances are significantly enhanced compared to those at other resonances. These changes are the results of desorption and surface reaction of the CCl_4–Si surface complex due to X-ray irradiation. We have demonstrated that state-specific enhancement of ion desorption can be successfully applied to characterize the reaction dynamics of adsorbates adsorbed on surfaces by X-ray irradiation.
© 2006 Elsevier B.V. All rights reserved.

Keywords: Photon stimulated ion desorption; Ion kinetic energy distribution; State-specific fragmentation; Synchrotron radiation

1. Introduction

The adsorption or surface mediated reaction of molecular adsorbates on semiconductor surfaces is of substantial importance not only for the basic understanding of the interfacial reaction dynamics but also for the potential application to microfabrication of material structure. With the on-going reduction in the dimensions of electronic device into the nanometer range, the understanding and control of X-ray-mediated monolayer and submonolayer reactions on surfaces is becoming more essential for the development of the evolving technology.

Active control of surface reaction using electromagnetic radiation is one of the key issues of surface photochemistry. It has been demonstrated that laser control of chemical reactions is promising approach to this goal [1]. Site-selective photon-induced chemical reactions via core excitation pro-

vide another approach to the active control of chemical reactions, because the microfabrication of material structure will require the control of very precisely localized reactions.

Selective desorption of specific species from molecular adsorbates following photoexcitation is an attractive topic in surface science. With the availability of tunable synchrotron radiation in the X-ray region, it is possible to excite selectively a specific atom or a specific site in molecules. Core electrons of an atom of particular element in a molecule can be excited into specific bound states below the ionization threshold. The site-specific fragmentation via core-level excitation was identified in several systems [2–10], but not observed in some molecules, such as $Fe(CO)_2(NO)_2$ [11]. The mechanisms of bond-selective fragmentation of molecules via core-level excitation are not fully understood and remain the subject of extensive research [12]. In addition, the investigation of chemical reactions of adsorbates on surfaces induced by bond-selective photofragmentation or X-ray irradiation is still scarce [13].

---

* Corresponding author.
  E-mail address: jmchen@nsrrc.org.tw (J.M. Chen).

Photon stimulated ion desorption (PSID) of molecules adsorbed on surfaces has been proven to be a very powerful technique for probing the surface reaction dynamics [14,15]. PSID of molecular adsorbates can provide insight into the local electronic structure, bonding geometry of the surface complexes, and the detailed information about the relevant ion desorption processes. Besides, the ion energy distribution of ion desorption for adsorbates on surfaces can provide the information on the desorption dynamics such as the steepness of potential energy surfaces of precursor excited states and the energy partitioning among the internal degree of freedom of fragments [16,17]. As known, the photoemission spectroscopy has been widely applied to characterize the products of surface reaction via photoexcitation [18]. However, the characterization of the reaction dynamics of adsorbates on surfaces by X-ray irradiation using the PSID technique is still very limited.

The comprehensive understanding of the interaction of Cl-containing compounds ($SiCl_4$, Si_2Cl_6, CCl_4, etc.) with silicon is of substantial importance in the semiconductor industry [19]. Molecules of this class are used in reactive ion etching of semiconductors. Adsorbed on single-crystalline surfaces, they are model systems for studies of surface photochemistry. In the present study, by combining the photon-stimulated ion desorption spectra, X-ray absorption spectra, and ion kinetic energy distribution measurements, X-ray initiated molecular photochemistry for CCl_4 and $SiCl_4$ adsorbed on Si(100) at $\sim$90 K following Cl 2p core-level excitation to various resonances has been investigated. The most striking observation is that the Cl $2p \rightarrow 8a_1^*$ excitation of solid $SiCl_4$ induces the significant enhancement of the Cl^+ yield, while the Cl $2p \rightarrow 7a_1^*$ excitation of condensed CCl_4 leads to a moderate enhancement of the Cl^+ yield. The enhancement of Cl^+ yield at the specific core-excited states is strongly correlated to the ion escaped energy. Besides, we have demonstrated that state-specific enhancement of ion desorption can be successfully applied to characterize the reaction dynamics of adsorbates adsorbed on surfaces by X-ray irradiation.

2. Experiments

The experiments were carried out at 6 m high-energy spherical grating monochromator (HSGM) beamline of the National Synchrotron Radiation Research Center (NSRRC) in Taiwan. All the data were collected using an ultrahigh-vacuum (UHV) chamber with a base pressure of $\sim$1 × 10^{-10} Torr. Before installation into the UHV chamber, the substrate Si(100) crystal was treated with hydrogen-peroxide-based immersion cleaning procedure to remove residual organic molecules and transition metals from cutting. After mounting the substrate in the UHV chamber, the Si(100) surface was cleaned by repeated resistive heating to $\sim$1100 °C under vacuum prior to the measurements. The high purity $SiCl_4$ and CCl_4 (Merck, 99.9%) were degassed by several freeze-pump-thaw cycles

before use. The vapor of $SiCl_4$ or CCl_4 was then condensed through a leak valve onto a Si(100) surface at $\sim$90 K.

The X-ray absorption spectra were recorded by the total-electron yield (TEY) mode using a microchannel plate detector. The ion desorption yields were detected with a quadrupole mass spectrometer (Balzers model QMA 410 with off-axis secondary electron multiplier). The ion kinetic energy distribution (not calibrated) was measured by a quadrupole mass spectrometer with a 45° sector field analyzer (Hiden, EQS). The quadrupole mass detector was oriented perpendicular to the substrate surface. Photons were incident at an angle of 45° with respect to the substrate normal. The incident photon intensity (I_0) was monitored simultaneously by a Ni mesh located after the exit slit of the monochromator. All the X-ray absorption spectra and PSID spectra were normalized to I_0. The photon energies were calibrated using known X-ray absorption transitions of the carbon contaminants on the optical surfaces of the monochromator. For the PSID measurements, the slits of HSGM beamline were set to 100 μm corresponding to the energy resolution of $\sim$0.3 eV at 200 eV. For ion energy distribution measurements, the slits of beamline were set to 150 μm.

All exposures are given in Langmuirs (1 L = 1 × 10^{-6} Torr s). The surface coverage was determined by thermal desorption spectroscopy (TDS). The TDS spectra from CCl_4/Si(100) show a single molecular desorption peak of $\sim$139 K with an exposure of 4 L or less. Above 4-L exposure, an additional peak starts appearing at a lower temperature of $\sim$132 K and its intensity increases with exposures. Thus, 4-L exposure of CCl_4 on Si(100) corresponds to one monolayer (ML). To ensure the reproducible data, the ion kinetic energy distributions were recorded from 15 L to 55 L exposure of $SiCl_4$ or CCl_4 on Si(100).

3. Results and discussion

In Fig. 1(a), the PSID spectra of $SiCl^+$, $SiCl_2^+$, $SiCl_3^+$, Si^+, and Cl^+ for $SiCl_4$ adsorbed on Si(100) at $\sim$90 K with multilayer coverage (>100-L exposure) following Cl 2p core-level excitation are reproduced. The Cl L_{23}-edge X-ray absorption spectrum for condensed $SiCl_4$ measured by the total electron yield (TEY) mode is also displayed for comparison. The absorption peaks labeled 1 and 1′ are assigned to the transition, Cl $2p \rightarrow 8a_1^*$. The features labeled 2 and 2′ correspond to the Cl $2p \rightarrow 9t_2^*$ excitations. Excitations to the Rydberg states are responsible for the absorption peaks labeled 3 and 4 [20]. The broad band at $\sim$216 eV labeled 5 is ascribed to the shape resonance.

As noted from Fig. 1(a), the PSID spectra of $SiCl^+$, $SiCl_2^+$, $SiCl_3^+$ and Si^+ show a close resemblance with the Cl L_{23}-edge X-ray absorption spectrum of solid $SiCl_4$. In contrast, the Cl^+ PSID spectrum exhibits a clear dissimilarity with the Cl L_{23}-edge X-ray absorption spectrum. The transition, Cl $2p \rightarrow 8a_1^*$, leads to a significant enhancement ($\sim$900%) in the Cl^+ desorption yield when compared to the transitions, Cl $2p \rightarrow 9t_2^*$ and Cl $2p \rightarrow$ Rydberg states. The
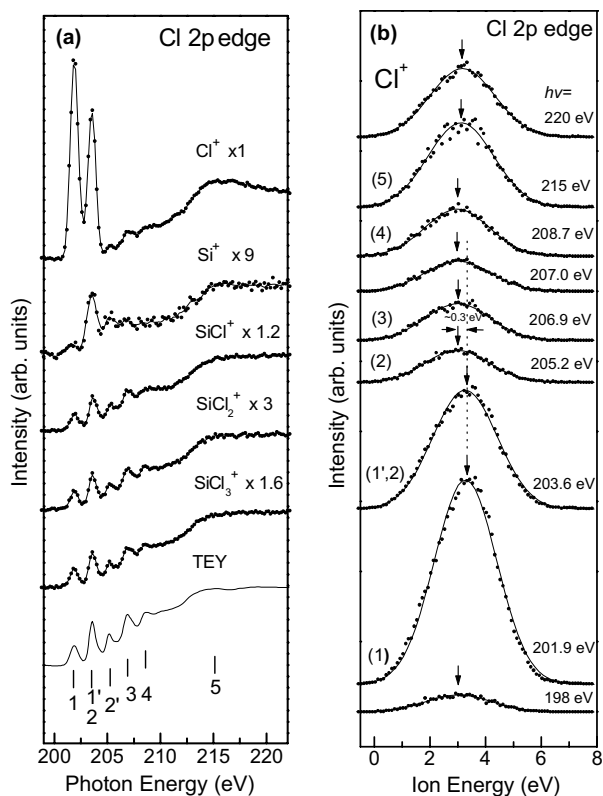
Fig. 1. (a) PSID spectra of Cl^+, Si^+, $SiCl^+$, $SiCl_2^+$, and $SiCl_3^+$ for condensed $SiCl_4$ (>100-L exposure) along with Cl L-edge TEY spectrum via Cl 2p core-level excitation. (b) Cl^+ ion energy distributions for $SiCl_4$ adsorbed on Si(1 0 0) at ~90 K following Cl 2p core-level excitation. The photon energy used for the excitation is indicated in each spectrum. The number indicated in each spectrum corresponds to absorption peak marked in the TEY spectrum in (a).
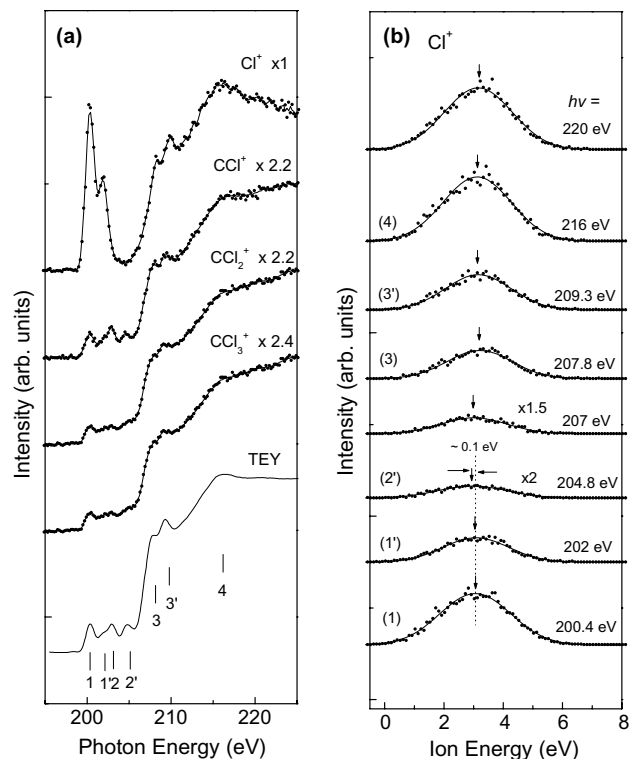

Fig. 2. (a) PSID spectra of Cl^+, CCl^+, CCl_2^+, and CCl_3^+, together with Cl L-edge TEY spectrum, for solid CCl_4 following Cl 2p core-level excitation. (b) Cl^+ ion energy distributions of condensed CCl_4 in the vicinity of Cl 2p edge. The photon energy used for the excitation is indicated in each spectrum. The number indicated in each spectrum corresponds to absorption peak marked in the TEY spectrum in (a).

Cl $2p_{3/2} \rightarrow 8a_1^*$ excitation (absorption peak labeled 1) in condensed $SiCl_4$ gives rise to ~900% enhancement of Cl^+ yield, as compared to the intensity ratio of corresponding transition to the shape resonance at ~216 eV in Cl L_{23}-edge X-ray absorption spectra. Even though these states are assigned to transitions from the same atomic site, there is a significant difference in efficiency for producing various ions. This infers that the character of core-excited states plays a vital role in the ion desorption processes.

Based on resonant photoemission studies, the spectator Auger and normal Auger transitions were the dominant decay channels for the excited Cl 2p core holes of condensed $SiCl_4$, producing the excited states with multiple holes in the valence orbitals [21]. Accordingly, a close resemblance of the PSID spectra and the Cl L-edge TEY spectrum of solid $SiCl_4$, as shown in Fig. 1(a), is attributed to the Auger decay of core-excited states and subsequent coulomb repulsion of the multi-valence-hole final states, which was called the Auger-initiated desorption (AID) mechanism [22,23].

In Fig. 1(b), the Cl^+ ion energy distributions of $SiCl_4$ adsorbed on Si(1 0 0) at ~90 K with multilayer coverage following Cl 2p core-level excitations are reproduced. As noted, the Cl^+ ion energy distributions via the Cl 2p → $8a_1^*$ excitation are shifted to higher energy (~0.3 eV) com-

pared to those via the Cl 2p → $9t_2^*$ and Cl 2p → shape resonance excitations. It is clear that, due to higher ion kinetic energy and consequently lower ion reneutralization rates, the Cl^+ yield via the Cl 2p → $8a_1^*$ excitation is significantly enhanced [24].

In Fig. 2(a), the PSID spectra of Cl^+, CCl^+, CCl_2^+, and CCl_3^+, along with X-ray absorption spectrum, for solid CCl_4 following Cl 2p core-level excitation are shown. The doublet structures labeled 1 and 1' correspond to Cl $2P_{3/2}$–Cl $2P_{1/2}$ spin-orbit splitting. The first doublet peaks labeled 1 and 1' in Fig. 2(a) are attributed to transitions from Cl 2p core states into the $7a_1^*$ C–Cl antibonding orbital. The next doublet structures labeled 2 and 2' correspond to excitations to the $8t_2^*$ C–Cl antibonding orbital [25]. The absorption peaks labeled 3 and 3' might originate from shake-up excitation (two-electron excitation) involving simultaneous excitation of a Cl 2p electron and a valence electron to unoccupied orbitals [26]. The broad peak labeled 4 is attributed to a shape resonance.

As noted from Fig. 2(a), the PSID spectra of CCl^+, CCl_2^+, and CCl_3^+ nearly follow the Cl 2p-edge TEY curve of solid CCl_4. In contrast, the Cl^+ PSID spectrum and the Cl 2p-edge TEY spectrum of condensed CCl_4 are clearly dissimilar. There exists a moderate enhancement of the Cl^+ yield at the Cl 2p → $7a_1^*$ resonant excitation, as compared to the Cl 2p → $8t_2^*$ excitation. The Cl

$2p_{3/2} \rightarrow 7a_1^*$ excitation (absorption peak labeled 1) in condensed CCl_4 gives rise to ~500% enhancement of Cl^+ yield, as compared to the intensity ratio of corresponding transition to the shape resonance at ~216 eV in Cl L_{23}-edge TEY spectrum. On the bases of the resonant photoemission spectra, Cl $2p \rightarrow 7a_1^*$ and Cl $2p \rightarrow 8t_2^*$ excitations proceed via primarily the LVV spectator Auger transition, which leads to the final electronic configuration of a two-hole, one-electron (2h1e) state. In addition, shake-up excitation and shape-resonance excitation are followed by normal Auger decay, leading to the two-hole (2h) final states. Accordingly, the close resemblance of PSID spectra the CCl^+, CCl_2^+, and CCl_3^+ with the Cl L_{23}-edge TEY spectrum for solid CCl_4 is attributed to the AID mechanism [27].

In Fig. 2(b), the Cl^+ ion energy distributions of condensed CCl_4 following Cl $2p$ core-level excitations are reproduced. As noted, the Cl $2p \rightarrow 7a_1^*$ excitation for condensed CCl_4 gives rise to an ion energy distribution higher (~0.1 eV) than the Cl $2p \rightarrow 8t_2^*$ excitation, but lower (~0.1 eV) than the Cl $2p \rightarrow$ shape resonance excitation. Accordingly, the Cl $2p \rightarrow 7a_1^*$ excitation only leads to a moderate enhancement of Cl^+ yield, as compared to the Cl $2p \rightarrow 8t_2^*$ and Cl $2p \rightarrow$ shape resonance excitations.

Besides such AID process, the ion desorption can be induced by the secondary electrons produced by X-ray irradiation, called X-ray induced electron-stimulated desorption (XESD) [28,29]. To clarify the contribution of the secondary electrons to positive-ion desorption, we have performed Cl^+ PSID spectra of CCl_4 on a Si(100) surface at ~90 K as a function of exposure (3 L–60 L), as shown in Fig. 3. As noted from Fig. 3, no notable spectral changes of
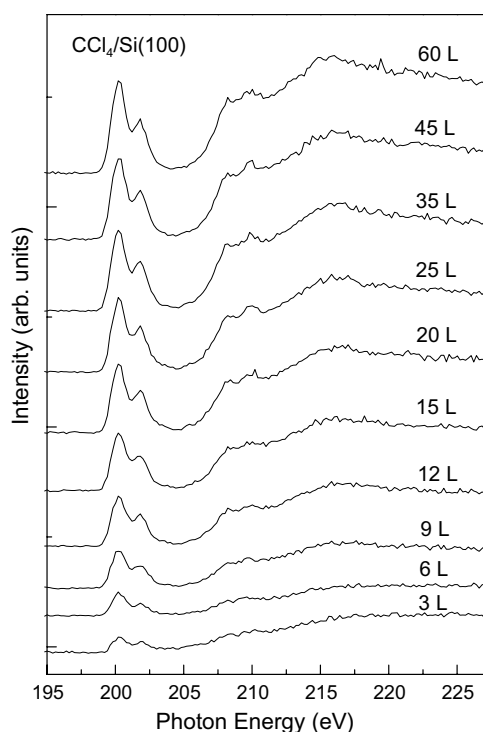

Fig. 3. Cl^+ photon stimulated ion desorption spectra of CCl_4 on a Si(100) surface at ~90 K as a function of exposure.

Cl^+ PSID spectra were observed as a function of coverage, particularly for multilayer coverages. It has been demonstrated that, when the Auger-initiated desorption process is active, contribution of the XESD process to positive-ion desorption is minor for thick layer [30,31]. The present result is consistent with this conclusion. Thus, for present thick-layer $SiCl_4$ or CCl_4 on Si(100) (>100-L exposure) in Figs. 1 and 2(a), the Auger-initiated desorption process would dominate over desorption channel induced by secondary electrons.

It is of great intriguing to compare the ion desorption between condensed $SiCl_4$ and CCl_4 following Cl $2p$ core-level excitation. As shown in Figs. 1 and 2(a), the enhancement of the Cl^+ yield via the Cl $2p \rightarrow 8a_1^*$ excitation of solid $SiCl_4$ is considerably higher than that via the Cl $2p \rightarrow 7a_1^*$ excitation of condensed CCl_4. In other words, other Cl $2p$-to-valence and Cl $2p$-to-Rydberg excitations of condensed CCl_4 and $SiCl_4$ give rise to the scarce enhancement of the Cl^+ yield. As noted from Figs. 1 and 2(b), the Cl^+ ion energy distribution via the Cl $2p \rightarrow 7a_1^*$ excitation of condensed $SiCl_4$ exhibit a higher energy (~0.2 eV) than that via the Cl $2p \rightarrow 8a_1^*$ excitation of condensed CCl_4. The enhancement of Cl^+ yield at the specific core-excited states is therefore strongly correlated to the ion escaped energy. This infers that the desorption of Cl^+ ion is enhanced by a specific core-to-valence excitation with higher ion kinetic energy distribution [6]. These results provide possible explanations why bond-selective fragmentation of molecules via core-level excitation was not observed in some systems [11].

In Fig. 4(a), X-ray irradiation dependence of a sequence of Cl^+ PSID spectra for CCl_4 adsorbed on Si(100) at ~90 K (20-L exposure) is reproduced following Cl $2p$ core-level excitation. The total photon exposure per area to X-ray is indicated in each spectrum which differs only by the amount of time. The Cl L-edge TEY spectrum for condensed CCl_4 is also displayed in Fig. 4(a) for comparison. As dosed, the Cl $2p \rightarrow 7a_1^*$ excitation leads to a moderate enhancement of the Cl^+ yield for CCl_4/Si(100). Upon X-ray exposure, the Cl^+ yields at the $7a_1^*$ resonances decrease and new structures labeled 3 and 3′ are observed at higher photon energies. These changes observed in Fig. 4(a) are the results of desorption and surface reaction of the CCl_4–Si surface complex due to X-ray irradiation [32]. Especially noteworthy is that the Cl^+ yields at resonances labeled 3 and 3′are significantly enhanced compared to those at other resonances. At high X-ray doses, when the surface reaction has near completion, the subsequent Cl^+ ion energy distributions are measured and displayed in Fig. 4(b). As noted from Fig. 4(b), the Cl^+ ion energy distributions at 3 and 3′ resonances are shifted to a higher energy (~0.3 eV) compared to those at other resonances. In addition, the peak positions at 3 and 3′ resonances in Fig. 4(a) is approximately the same as those labeled 1, 1′ of condensed $SiCl_4$ in Fig. 1(a). Accordingly, X-ray induced surface reaction of CCl_4/Si(100) might form the Si–Cl bonds in the surface, which leads to the strong
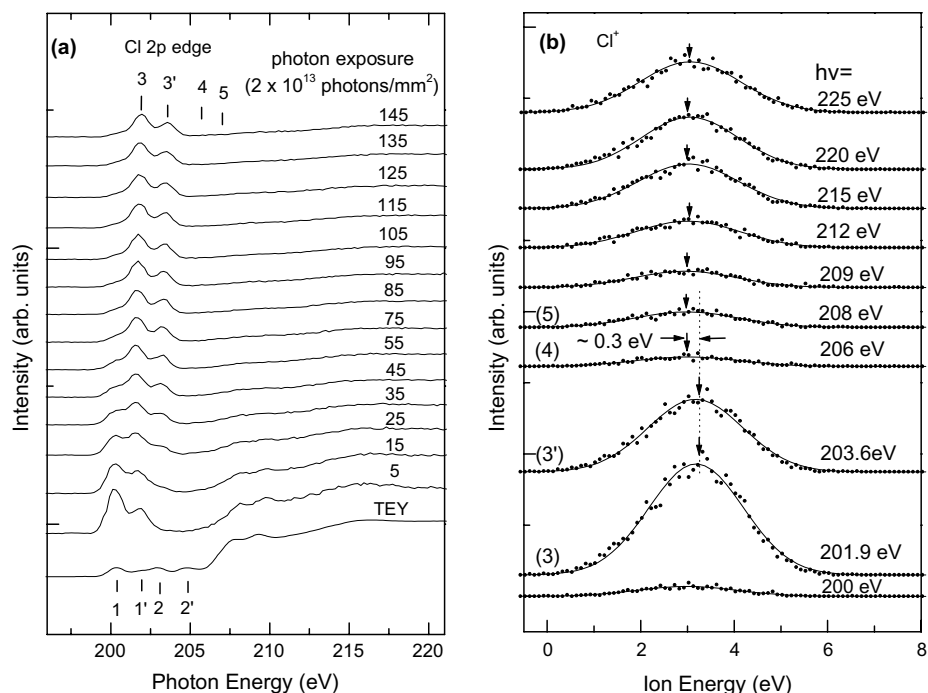
Fig. 4. (a) X-ray irradiation dependence of a series of Cl^+ PSID spectra for CCl_4 adsorbed on Si(100) at ∼90 K (20-L exposure) at the Cl 2p edge. The total photon exposure per area for each spectrum is given in units of ∼2×10^{13} photons/mm^2. (b) Cl^+ ion energy distributions for CCl_4/Si(100) at high X-ray doses, when the surface reaction has near completion. The number indicated in each spectrum represents excitation photon energy marked in the top of (a).

enhancement of the Cl^+ yields at 3 and 3′ resonances, as demonstrated in Fig. 1(a). A significant energy shift in Fig. 4(a) is due to the fact that the Cl 2p binding energies for the Si–Cl bonding are higher that those for the C–Cl bonding. As demonstrated, state-specific enhancement of ion desorption can be applied to characterize the reaction dynamics of adsorbates adsorbed on surfaces by X-ray irradiation.

4. Conclusion

We have investigated the X-ray induced molecular photochemistry for $SiCl_4$ and CCl_4 adsorbed on Si(100) at ∼90 K following Cl 2p core-level excitation by photon stimulated ion desorption and ion kinetic energy distribution measurements. The Cl^+ desorption yield shows a significant enhancement following the Cl 2p → $8a_1^*$ excitation of condensed $SiCl_4$, while the Cl 2p → $7a_1^*$ excitation for solid CCl_4 leads to a moderate enhancement of the Cl^+ desorption yield, The Cl^+ ion energy distribution via the Cl 2p → $7a_1^*$ excitation of condensed $SiCl_4$ exhibit a higher energy (∼0.2 eV) than that via the Cl 2p → $8a_1^*$ excitation of condensed CCl_4. The enhancement of Cl^+ yield at the specific core-excited states is strongly correlated to the ion escaped energy.

Upon X-ray exposure for CCl_4 adsorbed on Si(100), the Cl^+ yields at $7a_1^*$ resonances decrease and new structures at higher photon energies are observed. The Cl^+ yields at these new resonances are significantly enhanced compared

to those at other resonances. These changes are the results of desorption and surface reaction of the CCl_4–Si surface complex due to X-ray irradiation to form the Si–Cl bonds in the surface. We have demonstrated that state-specific enhancement of ion desorption can be successfully applied to characterize the reaction dynamics of adsorbates adsorbed on surfaces by X-ray irradiation.

Acknowledgements

References

[1] R.J. Levis, G.M. Menkir, H. Rabitz, Science 292 (2001) 709.
[2] W. Eberhardt, T.K. Sham, R. Carr, S. Krummacher, M. Strongin, S.L. Weng, D. Wesner, Phys. Rev. Lett. 50 (1983) 1038.
[3] R. Romberg, N. Heckmair, S.P. Frigo, A. Ogurtsov, D. Menzel, P. Feulner, Phys. Rev. Lett. 84 (2000) 374.
[4] Y. Baba, Low Temp. Phys. 29 (2003) 228.
[5] S. Nagaoka, K. Mase, M. Nagasono, S. Tanaka, T. Urisu, J. Ohshita, J. Chem. Phys. 107 (1997) 10751.
[6] J.M. Chen, K.T. Lu, J.M. Lee, C.I. Ma, Y.Y. Lee, Phys. Rev. Letters 92 (2004) 243002.
[7] T. Sekiguchi, H. Ikeura-Sekiguchi, Y. Baba, Surf. Sci. 454–456 (2000) 363.
[8] S. Nagaoka, J. Ohshita, M. Ishikawa, K. Takano, U. Nagashima, T. Takeuchi, I. Koyano, J. Chem. Phys. 102 (1995) 6078.

[9] N. Saito, J.D. Bozek, I.H. Suzuki, Chem. Phys. 188 (1994) 367.

[10] M.C.K. Tinone, K. Tanaka, J. Maruyama, N. Ueno, M. Imamura, N. Matsubayashi, J. Chem. Phys. 100 (1994) 5988.

[11] M. Simon et al., in: A. Beswick (Ed.), Synchrotron Radiation and Dynamic Phenomena, American Institute of Physics, New York, 1992, p. 323.

[12] Y. Baba, Low Temp. Phys. 29 (2003) 228, and references therein.

[13] S.P. Frigo, J.K. Simons, R.A. Rosenberg, J. Elec. Spectro. Rela. Phen. 80 (1996) 55.

[14] V. Rehn, R.A. Rosenberg, in: R.Z. Bachrach (Ed.), Synchrotron Radiation Research, Advances in Surface and Interface Science, vol. 1, Plenum, New York, 1992, p. 327.

[15] R.A. Rosenberg, V. Rehn, in: R.Z. Bachrach (Ed.), Synchrotron Radiation Research, Advances in Surface and Interface Science, vol. 2, Plenum, New York, 1992, p. 267.

[16] R. Weimar, R. Romberg, S.F. Frigo, B. Kassühlke, P. Feulner, Surf. Sci. 451 (2000) 124.

[17] J.M. Chen, K.T. Lu, J.M. Lee, J. Chem. Phys. 118 (2003) 5087.

[18] J.K. Simon, S.P. Frigo, J.W. Taylor, R.A. Rosenberg, Surf. Sci. 346 (1996) 21.

[19] J.J. Whitman, S.A. Joyce, J.A. Yarmoff, F.R. McFeely, L.J. Terminello, Surf. Sci. 232 (1990) 297.

[20] J.M. Chen, R. Klauser, S.C. Yang, C.R. Wen, Chem. Phys. Lett. 246 (1995) 285.

[21] J.M. Chen, K.T. Lu, Phys. Rev. Lett. 86 (2001) 3176.

[22] L. Knotek, P.J. Feibelman, Phys. Rev. Lett. 40 (1978) 964.

[23] P.J. Feibelman, Surf. Sci. 102 (1981) L51.

[24] J.M. Chen, K.T. Lu, J.M. Lee, J. Chem. Phys. 118 (2003) 5087.

[25] J.A. Tossell, J.W. Davenport, J. Chem. Phys. 80 (1984) 813.

[26] A.P. Hitchcock, C.E. Brion, Spectrosc. Relat. Phenom. 14 (1978) 417.

[27] J.M. Chen, R.G. Liu, S.C. Yang, Y.C. Liu, Y.P. Lee, Y.J. Hsu, C.-R. Wen, T.J. Chuang, J. Chem. Phys. 109 (1998) 8027.

[28] R. Jaeger, J. Stöhr, T. Kendellewicz, Surf. Sci. 134 (1983) 547.

[29] R. Jaeger, J. Stöhr, T. Kendellewicz, Phys. Rev. B 28 (1983) 1145.

[30] Y. Baba, K. Yoshii, T.A. Sasaki, Surf. Sci. 376 (1997) 330.

[31] J.M. Chen, S.C. Yang, Y.C. Liu, Surf. Sci. 391 (1997) 278.

[32] J.A. Yarmoff, A. Taleb–Ibrahimi, F.R. McFeely, Ph. Avouris, Phys. Rev. Lett. 60 (1988) 960.